Miniaturization of Planar Horn Motors

Stewart Sherrit, Patrick N. Ostlund, Zensheu Chang,
Xiaoqi Bao, Yoseph Bar-Cohen, Scott E. Widholm, Mircea Badescu

Jet Propulsion Laboratory, California Institute of Technology, Pasadena, CA 91109-8099

ABSTRACT

There is a great need for compact, efficient motors for driving various mechanisms including robots or mobility platforms. A study is currently underway to develop a new type of piezoelectric actuators with significantly more strength, low mass, small footprint, and efficiency. The actuators/motors utilize piezoelectric actuated horns which have a very high power density and high electromechanical conversion efficiency. The horns are fabricated using our recently developed novel pre-stress flexures that make them thermally stable and increases their coupling efficiency. The monolithic design and integrated flexures that pre-stresses the piezoelectric stack eliminates the use of a stress bolt. This design allows embedding solid-state motors and actuators in any structure so that the only macroscopically moving parts are the rotor or the linear translator. The developed actuator uses a stack/horn actuation and has a Barth motor configuration, which potentially generates very large torque and speeds that do not require gearing. Finite element modeling and design tools were investigated to determine the requirements and operation parameters and the results were used to design and fabricate a motor. This new design offers a highly promising actuation mechanism that can potentially be miniaturized and integrated into systems and structures. It can be configured in many shapes to operate as multi-degrees of freedom and multi-dimensional motors/actuators including unidirectional, bidirectional, 2D and 3D. In this manuscript, we are reporting the experimental measurements from a bench top design and the results from the efforts to miniaturize the design using 2x2x2 mm piezoelectric stacks integrated into thin plates that are of the order of 3 x 3x 0.2 cm.

Keywords: Actuators, Piezoelectric Motors, Rotary Devices, Horn Actuation, Barth motor

I. INTRODUCTION

Ultrasonic motors based on piezoelectric actuation have been available for some time[1,2,3]. The mode of operation, (quasi-static or resonant), type of motion (rotary or linear) and the shape of the actuation element (beam, rod, disk, etc.) can be used to classify the various piezoelectric motor configurations. Despite these distinctions, the fundamental principles of solid-state actuation are common to all of these devices. Each of these motor designs uses microscopic material deformations (associated with the excitation capability of piezoelectric materials) which are amplified through either quasi-static or dynamic/resonant means.

Motors and actuators are an important element of most mechanisms. The majority of actuators are based on electromagnetic rotary motors, such as DC, AC, brushed and brushless, etc. These types of motors use speed-reducing gears to compromise the speed, which can be as high as many thousands of RPM, in order to obtain higher torque. The use of a gear adds mass, volume and complexity as well as reduces the system reliability due the increase in number of the system components. The miniaturization of conventional electromagnetic motors is limited by manufacturing constraints and loss of performance efficiency. Potentially, rotary motors that are actuated by piezoelectric ceramics can offer an effective alternative for miniature-mechanisms[4]. These emerging motor technologies provide high torque density at low speed, high holding torque[5] , zero-backlash, simple construction, quiet operation and have a fast response time. They can also be made in annular through hole shapes for optical applications, electronic packaging and wiring through the center.

One of the first piezoelectric motor designs with significant rotational speeds discussed by Sashida[1] and originally published by Barth[6] is what is now known as the Barth Motor[7,8]. This device used extensional piezoelectric elements to produce a time varying force at a distance r from the center of a centrally supported disk as is shown in Figure 1. These micro-steps occur at a high frequency with the end result being macroscopic rotation of the rotor. The rotation direction is controlled by the choice of the actuators. This motor was reported to produce a significant torque however a measureable wear was noted during the motor operation and characterization. Another feature of these motors that is beneficial is their ability to be manufactured in a plane to produce compact low profile rotary motors. In this study we investigated the concept of using horns to produce macroscopic rotation and examined whether the piezoelectric ceramic

could be pre-stressed using flexures. For this purpose, we designed a set of horns that could be used to drive a rotor to perform useful work. The monolithic horns were manufactured using Titanium alloy (Ti-6Al-4V) and an electron beam melting/manufacturing process (EBM) by CALRAM Inc. In the EBM process the titanium parts can be made to an accuracy of about 0.4 mm with comparable strengths to as-cast and wrought materials[9]. The part quality is such that they are now used in both the aerospace and in medical implant fields. The EBM manufacturing approach is useful for small production runs. If larger production and cheaper cost per part is required, one could use an investment casting tree approach[10] where it is also possible to co-cast stainless steel and titanium. The piezoelectric stacks were purchased from Piezomechanik Gmbh in a bi-polar configuration with nominally 25.4 mm OD and 9.33 mm thick. Analysis of the small signal resonance data of the bare stack gave an effective piezoelectric constant of 480 pC/N for the material and a capacitance of 261 nF. The coupling was determined to be k_{33} =0.56 and the elastic compliance at constant field in the 33 direction was 5.4×10^{-11} m^2/N. The mechanical Q was in the 40 - 80 range. Initial testing of the motor with one horn demonstrated a rotor speed of 15 RPM with a torque of approximately 0.3 N-m could be produced[11]. The torque was determined by hanging a mass around the shaft, then measuring the constant rate at which the mass was lifted against gravity.

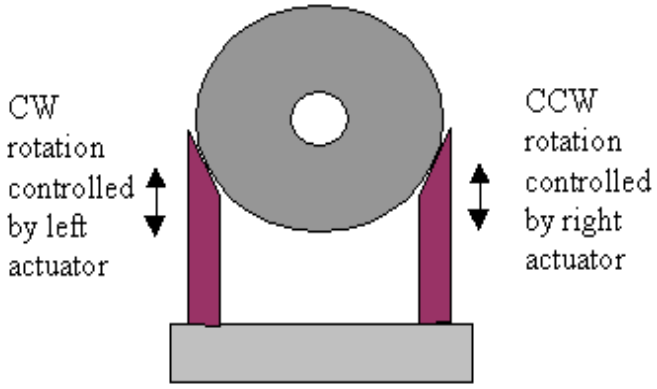

FIGURE 1: Schematic diagrams of a Barth Motor[6]

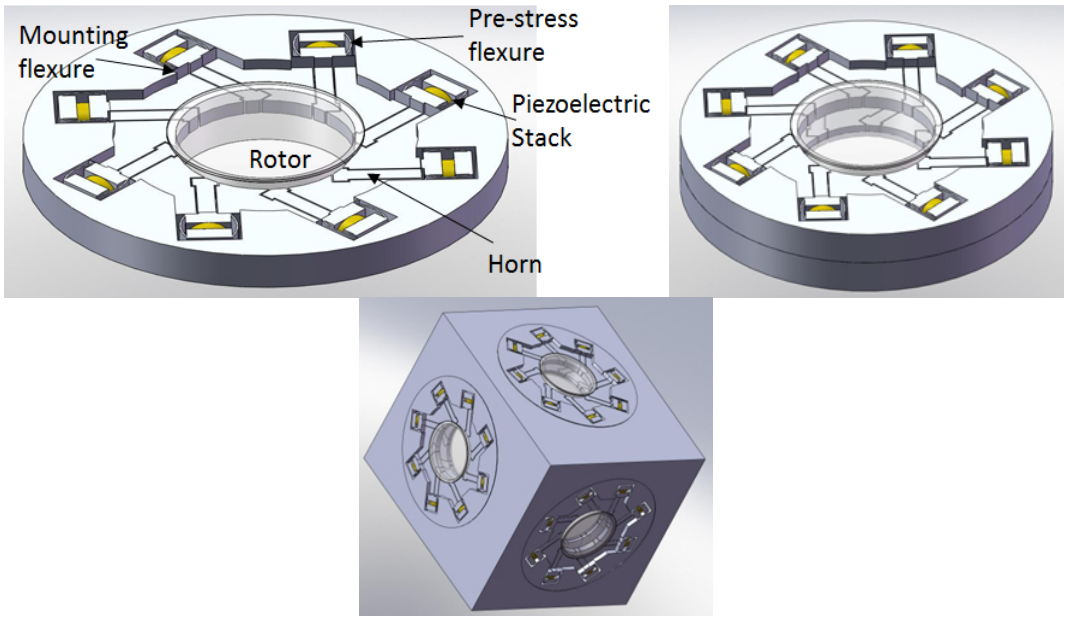

FIGURE 2: Novel Barth Motors designed for unidirectional, bidirectional and 3D operations.

The results of the initial flexure horn development[12] and the demonstration of a rotary motor led us to investigate the ability to produce planar structure where the motors could be embedded in the walls of specific structures. This

approach could have significant benefits in saving mass and volume for other critical components without degrading the overall structure and for the goal of miniaturization of electromechanical systems. The approach could also be used to increase the number of horns in the plan to multiply the torque or to stack the planes of horns to increase torque. The horns can also be arranged in counter positions to produce clockwise and counter clockwise rotation. Other arrangements include the ability to embed them in cubes or any other 3D object with limited curvature. The planar structure can be produced by standard manufacturing techniques such as milling, stamping, casting and EDM for very small structures. In this paper, we present the results of our modeling and testing of the large bench top planar motor shown in Figure 3 and 4 and the development on a miniaturized version that is of the order of 3x3 centimeters square and 2 mm thick.

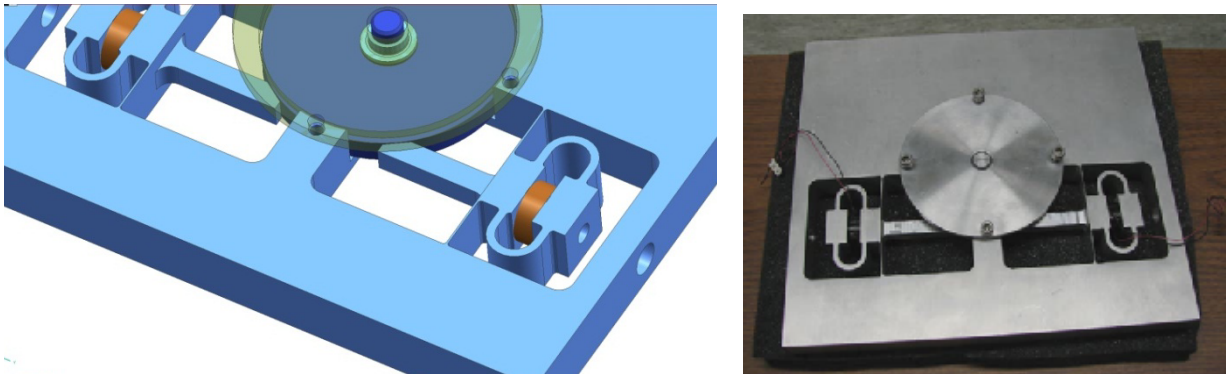

FIGURE 3: A CAD model of a prototype rotary motor that can drive a rotor clockwise and counter clockwise along with a photograph of finished motor. The preload on the rotor for each of the horns can be relieved by a bolt connected through the frame to the backing.

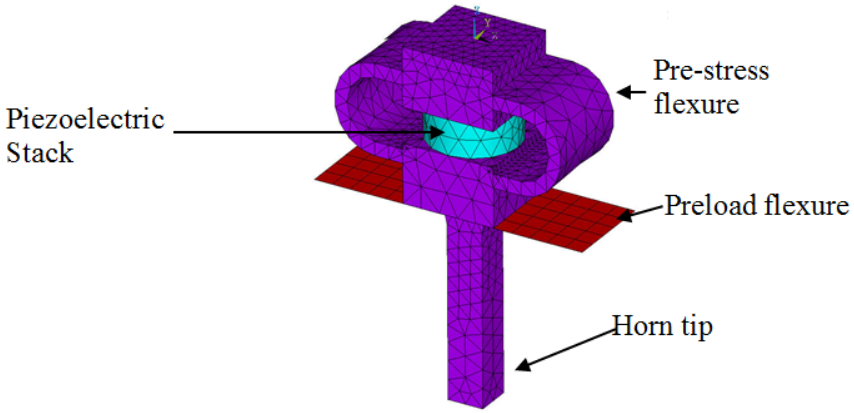

FIGURE 4: The ANSYS model used to model the horn actuators. Total number of nodes= 8753, Total number of elements=5017, Boundary condition: Edges of flexures fixed.

II. MODELLING AND EXPERIMENTS OF BENCHTOP PROTOTYPE

To test the planar motor structures a planar rotary bidirectional motor was designed and modeled using ANSYS. A CAD model and the assembled prototype motor are shown in Figure 3. The piezoelectric stacks are the same as the stacks that was used in the Barth motor having the monolithic horns discussed above (Piezomechanik Gmbh). The horn actuators of the prototype shown in Figure 3 were modeled in ANSYS to determine the resonance frequency, coupling and the position of the nodal plane. The isolated horn model is shown above in Figure 4 and resonator properties for two difference mounting flexures shown as red thin structures at the top of the horn-base in Figure 4 are listed in Table 1. The tip displacement, power and current as a function of frequency were determined for a 1 volt input AC signal and the peak results are given in Table 1.

Table 1: The resonator parameters for two mounting flexure thicknesses at 1 Volt peak excitation. The tip displacement and power and current are amplitude values.

Thickness (mm)	0.75	1.5
Resonance f (kHz)	23.6	23.9
Tip displacement (microns)	0.31	0.32
Coupling k (#)	0.20	0.19
Peak power(w)	0.096	0.101
Peak Current (A)	0.104	0.111
Adjacent modes (kHz)	22.9, 24.2	23.3, 24.0

The analysis suggests that at 20 Volts the theoretical peak tip displacement is about 6 microns and the power dissipated as actuation and heat will be of the order of 40 Watts assuming the displacement is linear in voltage and the power is quadratic in voltage. The speed and torque are a function of the friction on the rotor and depend on the normal forces of the rotor and base and the rotor and the counter driven horn. The rotary motor shown in Figure 3 was produced based on the horn analyzed (Figure 4) with a mounting flexure thickness of 1.5 mm and was fabricated using an end mill. The first extensional resonance (admittance spectra) for the two free horns is shown in Figure 5 and it is interesting to note the differences in their resonance spectra. Since the variability of their free piezoelectric stacks is much smaller, the large differences shown in Figure 5 are attributed to machining variability of the pre-stress and pre-load flexures. The pre-load flexures apply the force on the horn tip to the rotor and due to the thicknesss of these structures it is the most flexible and deformable element in the design. In assembling the motor, we managed to deform one of the flexures so that it was bowed out away from the rotor. The resonance frequency of the horn with the #11 piezoelectric stack was 22.9 kHz while the resonance frequency of the horn with #7 piezoelectric stack is 20.8 kHz. The difference is about 10% which is larger than expected. The difference in coupling was even more pronounced with the horn (#7) having a coupling of k = 0.36 and the number horn (#11) had a coupling of k = 0.23. The horn with the #11 piezoelectric stack matched the analysis results fairly closely as can be seen in Table 1 for the 1.5 mm preload flexure.

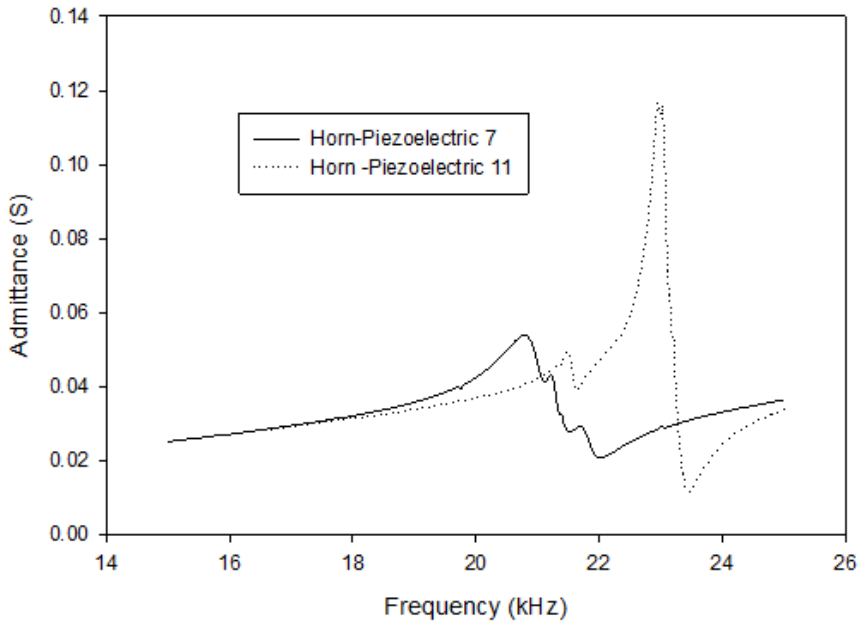

Figure 5: The admittance spectra of the two horns in the planar motor breadboard. The resonance of the piezoelectric stacks is much more consistent which suggests the fabrication tolerances are critical for this application.

The no load speed and the stall torque of the developed bench top prototype motor are shown in Figure 6 and 7. The stall torque for this motor was measured using a pulley and mass system on a scale. The stall torque was calculated from the weight the motor off-loaded from the scale during a run. The design was found to increase by almost a factor of two, after sandpaper (1500 grit) was applied to the rotor and the horn tip, as can be seen in Figure 7.

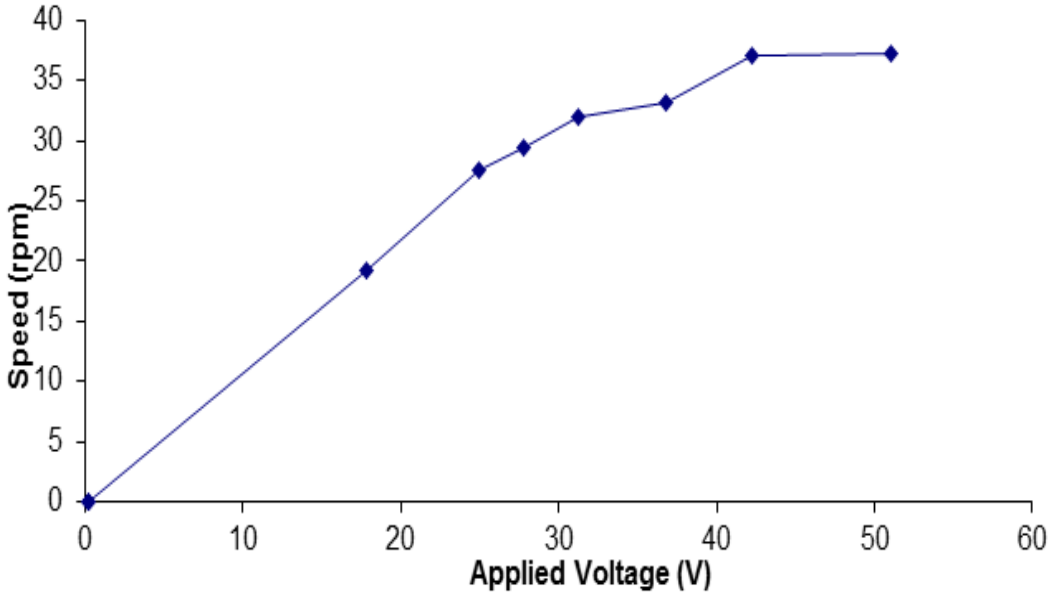

Figure 6: The no load speed of the motor as a function of the drive voltage to the horn.

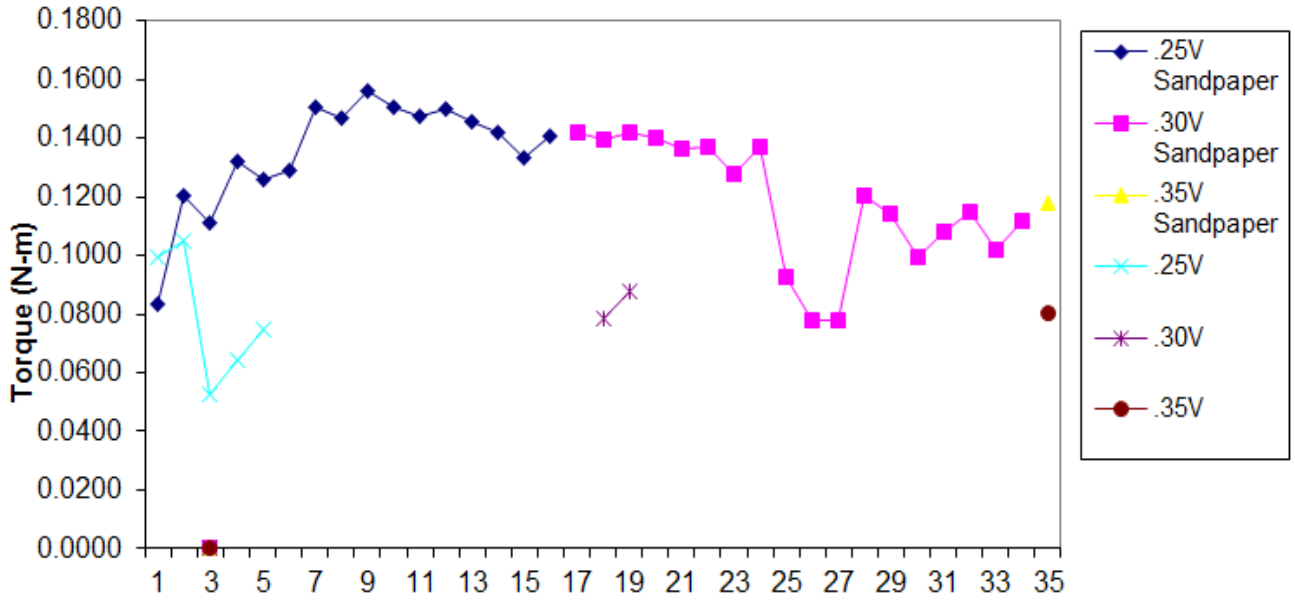

Figure 7: A series of measurements of the stall torque of the motor as a function surface treatment of the rotor and horn tip.

III. MODELLING AND EXPERIMENTS OF MINIATURE PROTOTYPE

The initial results of the bench top prototype guided the development of a miniature motor as shown in Figure 9. In the design of the miniature motor a decision was made to produce 4 horns all working in the same direction to enhance the torque density. The piezoelectric stacks (PICMA PL022.30) were nominally 2x2x2 mm (produced by PI Ceramic). The impedance spectra of the free resonance of the stacks are shown in Figure 8. The electromechanical coupling is k = 0.66. Two versions of the miniature planar motor were developed, one design with a volume of 33x33x2 mm, and another 38x38x2 mm.

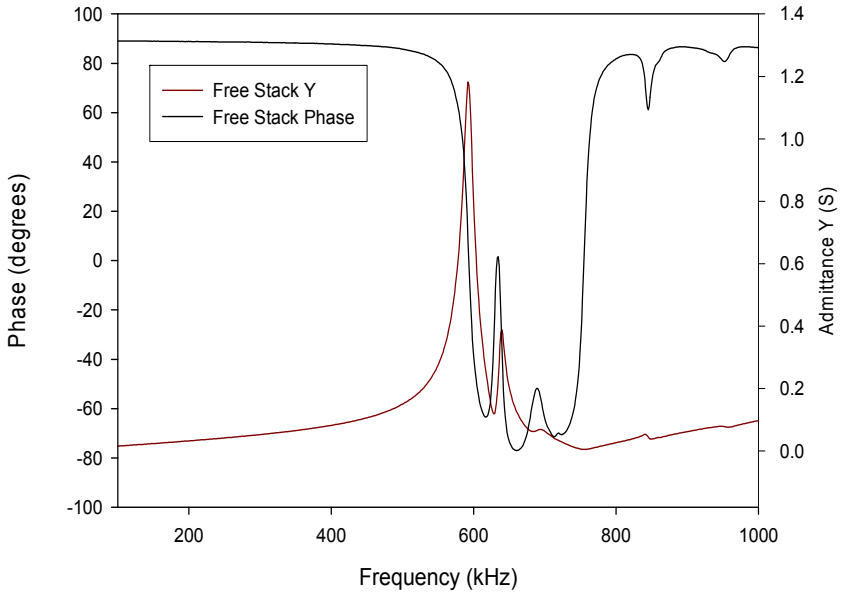

Figure 8: The free resonance of the 2x2x2 PICMA stacks (produced by PI Ceramic). The electromechanical coupling is k= 0.66

The horn design was analyzed in ANSYS for the case of the horn tips free with and without the rotor and rotor retainer mounted. The solid models are shown in Figure 9 with and without the rotor and retainment support.

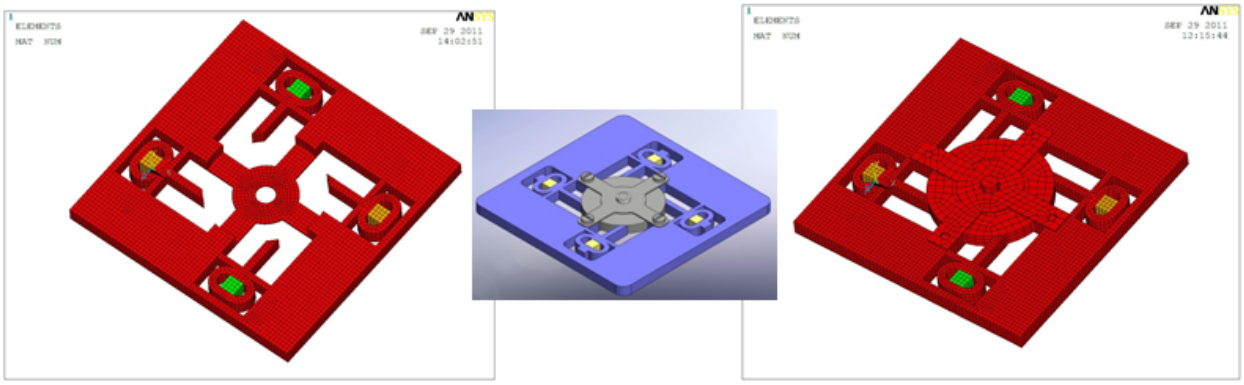

Figure 9: ANSYS and CAD models of the smaller planar motor design (33x33x2 mm)

The free horns were analyzed without the plate and the results are shown in Table 2.

Table 2: ANSYS results for standalone miniature horns

Actuator	Size (mm^2)	Length of Horn (mm)	Frequency (Hz)	Coupling Factor	Power (Watt)	Voltage	Tip disp (µm)
1	33X33X2	5.55	202935	0.25	1	1.86	1.38
2	38X38X2	8.05	157345	0.17	1	2.99	1.93

The resonance frequency for the small horn design was found to be 202.9 kHz and the horn coupling was calculated to be k = 0.25. The same analysis was done for the smaller horns mounted in the plate and the resonance frequency of the first mode was pushed up to 210 kHz. At 1 Watt the velocity of the rotor calculated at the no slip condition is 357 RPM with a torque of τ= 0.013 N-m. The density of modes seemed to increase as well with 4 modes appearing between

210 to 228 kHz. The coupling remained unchanged at k = 0.25. The impedance spectra of the horns without the rotors are shown in Figure 10.

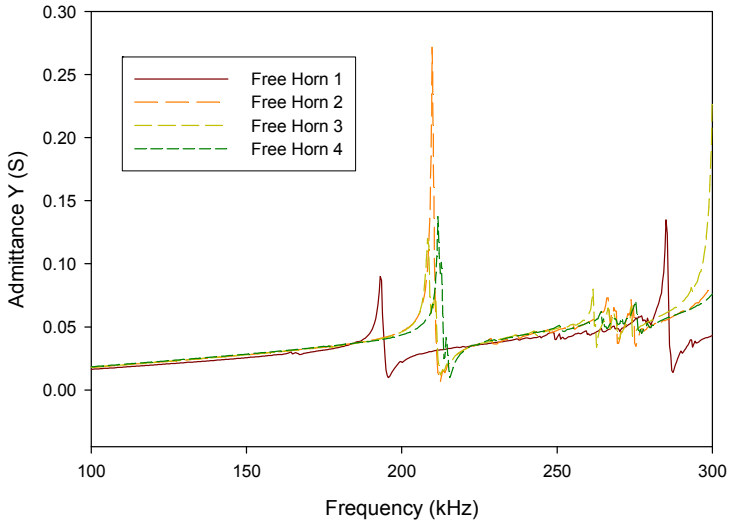

Figure 10: The impedance spectra for the free horns shown in the CAD model (left figure in Figure 9).

The predicted resonance frequency from ANSYS ranges from 210 kHz to 228 kHz with a coupling of k = 0.25 depending on the mode. The measured resonance frequency of the first resonance from Figure 10 ranges from 208.3 kHz to 211.7 kHz for horns numbered #2-4 and was 193.1 for horn #1. The coupling ranged from k = 0.17 to 0.22. The reason for the 10% drop in frequency for the #1 horn is currently unknown. The same admittance- frequency spectra were taken with the rotor with bushing and alignment fixture attached to the plate and the spectra are shown in Figure 11. It is apparent from the spectra that the extensional mode of the horn is obscured by multiple resonances in the horn/rotor structure. The transducer was assembled as shown in Figure 11 and the impedance spectra were measured again with the horns contacted to the rotor. The data is shown in Figure 12. The spectra show that all of the first extensional modes shifted up and the spectra become much noisier. The spectra for the # 1 horn are shifted to about 205 kHz while the other resonances are shifted to above 225 kHz and are very noisy. The spectra shown in Figure 12 indicated that as designed the rotor would not work. We connected all 4 piezoelectric horns to a function generator and applied an AC signal between 180 kHz and 300 kHz to try to excite the motor to no avail. The spectra in Figure 12 suggests that a lot of coupling to the rotor it taking place and that we need to reduce the excitation of possible radial modes in the rotor or even horn to horn coupling. We are currently looking at the potential to redesign the rotor to dampen out these reverberations.

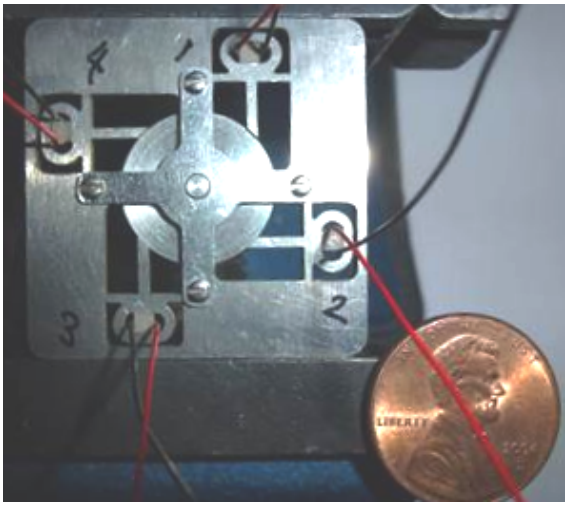

Figure 11: Photograph of the fabricated miniature planar motor along with a penny for scale. Four PZT ceramics stacks are shown in the flexures at the bottom of the horn.

One test that we plan to do is to change the rotor material from Aluminum (6061-T6) to Titanium, Stainless steel or possibly Teflon. Another idea to decouple the impacts from the disc of the rotor is to introduce an o-ring between the inner rotor and an outer ring where the horns contact.

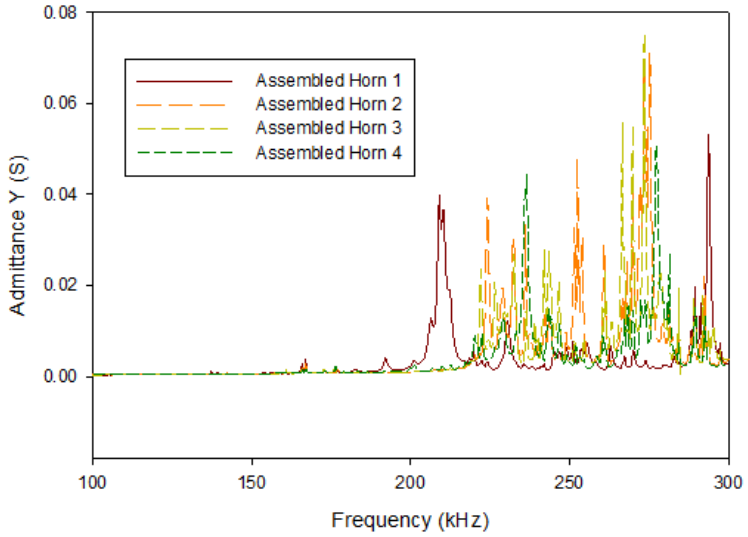

Figure 12: The impedance spectra for the horns with the rotor mounted as shown in the photograph (Figure 11). The spectra have been shifted up and are very noisy.

CONCLUSIONS

In this paper, we reported on designs based on a new approach to imbed actuation elements in the wall of a structure. In the initial tests, we demonstrated a Barth motor design using monolithic ultrasonic horns. We then demonstrated on a lab bench model that the motor elements could be embedded in a planar structure in the wall of a plate. The tests on this un-optimized motor demonstrated speeds up to 40 RPM and torques up to $\tau = 0.17$N-m. The ability to pre-stress the piezoelectric stacks using flexures has allowed for the design of simple horn structures that can be manufactured using standard fabrication techniques such as milling, stamping, casting and EDM for very small structures. The initial lab bench prototype planar design was scaled down to 33x33x2 mm using new 2x2x2 mm stacks (made by PI Ceramic). Initial FEM analysis of the planar horns predicted a resonance frequency of 211 kHz with a tip displacement of 1.38 microns at 1 watt peak excitation. The no slip speed was calculated to be about 357 RPM. The miniature planar motor with 4 horns was fabricated using EDM and assembled. Although the free horn data from the planar motor design matched the finite element predictions the resonance data (Admittance spectra) for the assembled motor including rotor shifted the resonance frequencies up and became quite noisy. It is suggested that this result was due to coupling of the rotor to the horns. Approaches including redesigning the rotor were discussed.

ACKNOWLEDGMENTS

Research reported in this manuscript was conducted at the Jet Propulsion Laboratory (JPL), California Institute of Technology, under a contract with National Aeronautics Space Administration (NASA), and was funded by the Army's RCTA2011 program. Reference herein to any specific commercial product, process, or service by trade name, trademark, manufacturer, or otherwise, does not constitute or imply its endorsement by the United States Government or the Jet Propulsion Laboratory, California Institute of Technology.

REFERENCES

[1] Sashida T., Kenjo T (1993): An Introduction to Ultrasonic Motors, Claredon Press , Oxford
[2] Ueha S., Tomikawa Y.(1993): Ultrasonic Motors, Claredon Press, Oxford

[3] Uchino K. (1996): Piezoelectric Actuators and Ultrasonic Motors (Electronic Materials--Science & Technology, 1), Kluwer Academic Pub; ISBN: 0792398114

[4] Hollerbach J.M., Hunter I.W. Ballantyne J. (1991):"A Comparative Analysis of Actuator Technologies for Robotics." In Robotics Review 2, MIT Press, Edited by Khatib, Craig and Lozano-Perez

[5] Flynn, A. M., Tavrow L.S., Bart S.F., Brooks R.F., Ehrlich D.J., Udayakumar K.R.,Cross L.E. (1992): "Piezoelectric Micromotors for Microrobots" J. of MEMS, **1**, No. 1, pp. 44-51

[6] Barth H.V. (1973):Ultrasonic Driven Motor, IBM Technical Disclosure Bulletin, **16**, pp. 2263

[7] Uchino K. , "Piezoelectric Ultrasonic Motors: Overview", Smart Materials and Structures, **7**, pp. 273-285, 1998

[8] Jin Jiamei, Zhao Chunsheng, " A vibrators alternation stepping ultrasonic motor" Ultrasonics **44**, pp. e565-e568, 2006

[9] CALRAM - http://www.calraminc.com/projects.htm
Downloaded Sept 1st, 2010

[10] RAMCAST- http://www.ramcast.com/ see sub-directory pdf/Ti2%20Conference%20paper.pdf downloaded Sept 1st 2010

[11] Stewart Sherrit, Xiaoqi Bao, Mircea Badescu, Daniel Geiyer, Phillip Allen, Patrick Ostlund, Yoseph Bar-Cohen, "Planar rotary motor using ultrasonic horns", Proceedings of the SPIE Smart Structures and Materials conference, Volume 7981, paper 22, San Diego, CA, 2011

[12] Stewart Sherrit, Xiaoqi Bao, Mircea Badescu, , Phillip Allen, Yoseph Bar-Cohen, "Monolithic Rapid Prototyped Flexured Ultrasonic Horns", Proceedings of the IEEE International Ultrasonics Symposium, pp. 886-889 , Presented in San Diego, CA, October 2010